Two-axis-twisting spin squeezing by multipass quantum erasure

Mingfeng Wang,[1,2,*] Weizhi Qu,[1] Pengxiong Li,[1] Han Bao,[1] Vladan Vuletić,[3] and Yanhong Xiao[1,4,†]

[1]*Department of Physics, State Key Laboratory of Surface Physics and Key Laboratory of Micro and Nano Photonic Structures
(Ministry of Education), Fudan University, Shanghai 200433, China*
[2]*Department of Physics, Wenzhou University, Zhejiang 325035, China*
[3]*Department of Physics, MIT–Harvard Center for Ultracold Atoms, and Research Laboratory of Electronics,
Massachusetts Institute of Technology, Cambridge, Massachusetts 02139, USA*
[4]*Collaborative Innovation Center of Advanced Microstructures, Nanjing 210093, China*

Many-body entangled states are key elements in quantum information science and quantum metrology. One important problem in establishing a high degree of many-body entanglement using optical techniques is the leakage of the system information via the light that creates such entanglement. We propose an all-optical interference-based approach to erase this information. Unwanted atom-light entanglement can be removed by destructive interference of three or more successive atom-light interactions, leaving behind only atom-atom entanglement. This quantum erasure protocol allows implementation of spin squeezing with Heisenberg scaling using coherent light and a cold or warm atomic ensemble. Calculations show that a significant improvement in the squeezing exceeding 10 dB is obtained compared to previous methods, and substantial spin squeezing is attainable even under moderate experimental conditions. Our method enables the efficient creation of many-body entangled states with simple setups and, thus, is promising for advancing technologies in quantum metrology and quantum information processing.

I. INTRODUCTION

Many-body entangled states of atoms are at the heart of quantum information processing [1–3] and quantum metrology [4–6], of which squeezed spin states (SSSs) form an important category. SSSs show fewer quantum fluctuations along a certain direction than the atomic-shot-noise limit [7] and, therefore, have attracted considerable interest recently since many precision measurements can now reach the atomic-shot-noise limit. Also, spin squeezing can serve as a criterion to quantify many-body entanglement [8]. A widely used approach to create such states is to let atoms interact with a common mode of light, as demonstrated in a variety of systems including cavities [9–11], cold atoms [12–15], and vapor cells [3]. In the majority of current experiments, SSSs are conditioned on a measurement. However, from a fundamental point of view, fully determined squeezed states, created in an unconditional way and with maximal entanglement, are still highly desirable. For this, new techniques are needed that allow complete control of the quantum noise of atoms and light.

A central problem hindering the achievement of a high degree of entanglement by light-mediated atom-atom interaction is the leakage of atomic spin information via the light exiting to the environment, which makes the squeezing process nonunitary and results in mixed states of the atoms with less squeezing. For instance, in the ground-breaking proposal of a general spin-squeezing scheme pioneered by the Takahashi group [16], the performance is limited by the unwanted atom-light entanglement created during the squeezing. One way to erase such entanglement is by using quantum control [17], where homodyne detection of the probe

optical pulse entangled with the atoms followed by feedback control can prevent information leakage and, thus, enhance the amount of achievable squeezing. An alternative approach is based on an optical cavity [9]. Although these existing erasure protocols can in principle realize a unitary process, they require either near-unity-quantum-efficiency detection or low loss [9,17], which makes their experimental implementation formidable.

Another outstanding problem in spin squeezing is the lack of simple approaches for unitary two-axis-twisting (TAT) spin squeezing. So far, one-axis-twisting (OAT) and quantum nondemolition detection have been realized, but without reaching the Heisenberg limit. As pointed out in Ref. [7], TAT promises squeezing to the Heisenberg limit, but it is challenging to design an experimentally realistic interaction process for realizing such a Hamiltonian. Indeed, so far, only a few theoretical proposals exist [18–22], and most of them either require special experimental systems such as a Bose-Einstein condensates or Rydberg atoms or need accurate multiple-pulse sequences. Therefore, to date, two-axis-twisted SSSs based on entanglement between atoms (instead of internal spin [23]) have not been experimentally achieved.

Here, we propose an all-optical interference-based approach to manipulate the quantum noise of atoms and light, which provides a novel yet experimentally feasible way to implement quantum erasure and enables a new scheme for TAT spin squeezing. Our method employs the interference of three atom-light interactions, canceling entanglement between the atoms and the output light, but keeping the effective nonlinear interaction between atoms. Such a quantum erasure does not use detection or feedback, is loss tolerant, and is experimentally feasible. Our scheme does not have special experimental requirements and involves only an ordinary polarized coherent laser beam under off-resonant Faraday interactions with an ensemble of warm or cold atoms. We note
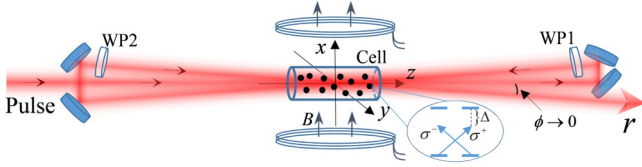
---

*mfengwang@aliyun.com

†yxiao@fudan.edu.cn

FIG. 1. Schematic of the proposed setup for two-axis-twisting spin squeezing. A light pulse passes three times through an atomic ensemble placed in a magnetic field, with its polarization rotated by wave plates between the passes. The light exiting the system contains no information about the atomic spin, and the atomic spin is perfectly squeezed. See text for details.

that other multipass schemes have been discussed for quantum memory applications [2,24], but not for spin squeezing.

II. MODEL AND BASIC INTERACTION

We consider off-resonant interactions between the collective spin of an ensemble of identical atoms $\mathbf{J} = (J_x, J_y, J_z)$ and a coherent light pulse [1,2]. The spin components satisfy the usual angular momentum commutation relations $[J_y, J_z] = iJ_x$ and obey Heisenberg's uncertainty relation, $(\Delta J_y)^2 \cdot (\Delta J_z)^2 \geqslant |\langle J_x \rangle|^2/4$. For simplicity we assume the ground-state atom to be a spin-1/2 system (see Fig. 1). Before interacting, the atomic spins are polarized along the x axis, forming a coherent spin state with mean values $\langle J_x \rangle = N_{at}/2, \langle J_y \rangle = \langle J_z \rangle = 0$ and variances $(\Delta J_y)^2 = (\Delta J_z)^2 = |\langle J_x \rangle|/2 = N_{at}/4$, as shown in Fig. 2(a), (i). Such a state will
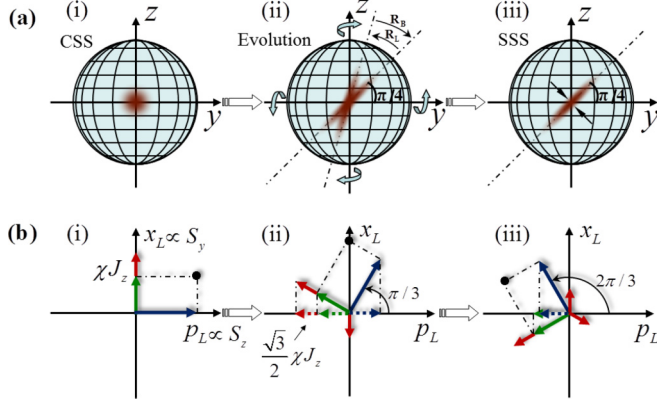

FIG. 2. (a) Illustration of the spin distribution's evolution on the Bloch sphere for the proposed triple-pass scheme. (i) The atomic state is initially prepared in the coherent spin state. (ii) The atom-light interaction induces two effects. First, it squeezes the spin uncertainty along the $3\pi/4$ direction. Second, it rotates the transverse spin around the x axis at a rate R_L, which can be compensated by the Larmor precession R_B, leading to the net effect (iii). (b) Phase-space portrait of the light's evolution induced by spin-light interactions. (i) During the V_1 interaction, x_L ($\propto S_y$) picks up atomic noise J_z. (ii) After a rotation produced by WP1 of the phase space with an angle $\pi/3$, the V_2 interaction imprints the atomic noise $-J_z$ onto the x_L quadrature. (iii) After another $\pi/3$ rotation by WP2, x_L "sees" J_z again. The sum of the three atomic spin contributions to the polarization of the light is 0, thereby canceling the spin-light entanglement. Dashed arrows are projections of all the vectors onto the p_L axis as explained in the text.

be squeezed according to the Wineland criterion [25] if

$$\xi^2 = \frac{N_{at}(\Delta J_\theta)^2}{|\langle J_x \rangle|^2} < 1, \qquad (1)$$

where $J_\theta = J_z \cos\theta - J_y \sin\theta$ with $\theta \in [0, 2\pi]$. The input light pulse is composed of a strong x-polarized component with carrier frequency $\omega_0 = 2\pi c/\lambda$ and a weak quantum component polarized along the y direction. The y-polarized component is relevant here and, in the narrow frequency band limit, can be described by spatially localized modes [26] $x_L(r) = \frac{1}{\sqrt{4\pi}} \int_b d\omega (a_y e^{-i(\omega_0-\omega)r/c} + \text{H.c.})$, $p_L(r) = -\frac{i}{\sqrt{4\pi}} \int_b d\omega (a_y e^{-i(\omega_0-\omega)r/c} - \text{H.c.})$ with commutation relations $[x_L(r), p_L(r)] = ic\delta(r - r')$, where the spatial argument r denotes the distance along the optical path, a_y is the annihilation operator for y-polarized photons, b is the bandwidth of the pulse, c is the speed of light, and the delta function has width c/b. Note that x_L (p_L) is in fact proportional to the Stokes vector $S_y(S_z)$ on a Poincaré sphere [1]. The quantum component is initially in a vacuum state such that $\langle x_L(r) \rangle = \langle p_L(r) \rangle = 0$, $\langle x_L(r)x_L(r') \rangle = \langle p_L(r)p_L(r') \rangle = ic\delta(r - r')$. If the light pulse propagates along the z axis and is tuned far off the atomic resonance, the forward scattering process in a one-dimensional model is described by the Faraday-type Hamiltonian [2,26]

$$V_1 = \frac{\hbar\chi}{\sqrt{T}} J_z p_L(r = 0) \propto J_z S_z, \qquad (2)$$

where the dimensionless coupling constant is given by $\chi^2 = \eta\alpha_0/2N_{at}$, with the decay parameter $\eta = N_{ph}\sigma\Gamma^2/A\Delta^2$ and the optical depth (OD) on resonance $\alpha_0 = N_{at}\sigma/A$. Here N_{ph} is the overall photon number of the pulse with duration T, σ is the scattering cross section, Γ is the natural line width (HWHM) of the atomic transition, A is the effective beam cross section, Δ is the detuning from the optical transition, and the sample is assumed to be located at $r = 0$.

The key physics of the Hamiltonian $J_z S_z$, (2), can be summarized as follows: For light propagating along z, the Stokes vector precesses around the z axis at a rate proportional to the atom spin J_z. If the light is x polarized ($S = S_x$), then its S_y component will pick up the atoms' J_z information. Similarly, if atoms are polarized along x, under evolution governed by this Hamiltonian, their J_y component will pick up the light's S_z information. Therefore, the atoms and light act as a quantum data bus for each other.

III. WORKING PRINCIPLE OF QUANTUM ERASURE

With the above physical picture, the principle of our three-pass interference-based quantum erasure can be understood. As shown in Fig. 1, an x-polarized light pulse propagates along z and passes through the atomic sample three times, with its quantum components (in the y-z plane of the Poincaré sphere) rotated by two wave plates (WP1 and WP2) between passages. From Hamiltonian (2), one readily derives, for a single pass, the input-output relations [2], $x_L^{out} = x_L^{in} + \chi J_z^{in}, p_L^{out} = p_L^{in}, J_y^{out} = J_y^{in} + \chi J_x p_L^{in}$, and $J_z^{out} = J_z^{in}$, where $x_L^{in,out}$ and $p_L^{in,out}$ are the normalized light quadrature, defined as $q_L^{in} = (1/\sqrt{T}) \int_0^T d\tau q_L(-c\tau, 0)$,

$q_L^{\text{out}} = (1/\sqrt{T}) \int_0^T d\tau q_L(cT - c\tau, T)$ with $q \in \{x, p\}$, and for the atomic spin $\mathbf{J}^{\text{in}} = \mathbf{J}(0)$, $\mathbf{J}^{\text{out}} = \mathbf{J}(T)$. One can see that after one interaction, the x quadrature (S_y) of the outgoing field now carries information about J_z. Then we assume that the Stokes vector is rotated by WP1 around the x-axis of the Poincaré sphere before interacting with the sample again. If the polarization rotation is $90°$, then after the second pass, $J_y^{\text{out}'} \simeq J_y^{\text{in}} + \chi J_x(x_L^{\text{in}} + p_L^{\text{in}}) + \chi^2 J_x J_z$, $J_z^{\text{out}'} = J_z^{\text{in}}$. At this stage, the result of the two-passage interaction is exactly the same as the previous double-pass (DP) scheme, which realizes nonunitary one-axis-twisting squeezing [16]. On the one hand, light picks up the atomic information J_z and imprints it onto J_y, inducing an OAT nonlinear spin dynamics represented by the $J_x J_z$ term; but on the other hand, light leaves its quantum noise (that is, $x_L + p_L$) imprinted on the atoms, producing unwanted entanglement between the light and the atoms, which prevents the realization of an ideal one-axis twisted state and greatly reduces the amount of achievable squeezing [16]. An immediate solution is to perform a projection measurement of the exiting light followed by an electronic feedback control [17]. Instead, here we propose disentangling the collective spin and light in a purely optical way by adding a third interaction. The essential idea is to appropriately adjust the light polarizations (only their quantum components) between passes so that the spin-light entanglement created by all passes destructively *interferes*, leaving only the net effect—a nonlinear OAT of the collective spin, $\propto J_z^2$. Therefore, the quantum erasure is built into the interaction.

We describe the choice of the polarization rotation angles between passes using the vector plots [Fig. 2(b)], where we consider the evolution of a point in the phase space of light (also on the Poincaré sphere). From the light's point of view, it experiences the atoms' collective spin three times successively, and according to the $J_z S_z$ Hamiltonian, atomic information equal to χJ_z (solid red arrow) is added to x_L ($\propto S_y$) each time, as depicted separately by the three plots in Fig. 2(b). The second pass picks up noise $-\chi J_z$ since the light propagation direction is reversed. If the Stokes vector is rotated by $60°$ between each interaction, then after the third interaction, the three solid red arrows add up to 0 [Fig. 2(b), (iii)], it means that the light exits without containing any information about the atomic spin. From the atom's point of view, in each pass, its J_y component obtains noise from the S_z component (p_L) of the light, as indicated by dashed arrows on the p_L axis in Fig. 2(b). If we sum up all the p_L (S_z) vectors from the three panels in Fig. 2(b), with a minus sign for the second passage (again, due to the reversed light prorogation direction), it can be seen that only the component proportional to χJ_z [dashed red arrow in (ii)] is left. This fact that the atoms' J_y component is displaced by an amount $\frac{\sqrt{3}}{2} \chi J_z$ indicates exactly the dynamics governed by the J_z^2 OAT Hamiltonian.

IV. IMPLEMENTATION OF A UNITARY TWO-AXIS-TWISTING SPIN SQUEEZING

The above scheme for the unitary OAT Hamiltonian J_z^2 can be extended to a TAT spin-squeezing scheme. First, one can write $J_z^2 = (J_z^2 - J_y^2)/2 + (J_z^2 + J_y^2)/2$, where the first term refers to the TAT transformation, which creates pure

squeezing with exponential growth along the $3\pi/4$ direction of the YZ plane [Fig. 2(a), (ii)], and the second term makes the transverse spin components rotate around the x axis (denoted R_L), which causes the unwanted swirling effect [7]. Next, the spin dynamics induced by this second term is $\dot{J}_y = (J_x J_z + J_z J_x)/2 \simeq N_{\text{at}} J_z/2$, $\dot{J}_z = -(J_x J_y + J_y J_x)/2 \simeq -N_{\text{at}} J_y/2$, which indicates $(J_z^2 + J_y^2)/2 \simeq -N_{\text{at}} J_x/2$. Therefore, a constant magnetic field in the x direction can impose an opposite Larmor precession R_B with respect to R_L and, thus, cancel the light-induced rotation, leading to a pure TAT spin state [Fig. 2(a), (iii)].

We now describe formally the creation of the two-axis-twisted spin state. Our TAT scheme (Fig. 1) relies on the near-simultaneous passage of a light pulse for three times through the atomic sample, placed in a homogeneous magnetic field. The pulse's spatial length is assumed to be much longer than the loop length between mirrors so that the laser pulse encounters itself in the cell. Such overlap is key to the current scheme, since (see below) it allows a continuous light-induced rotation R_L, which can then be instantaneously eliminated by the magnetic field, enabling a one-step realization of TAT. We note that pulse overlap is not necessary for the above unitary OAT scheme. After the first pass, WP1 (with the optical axis along the x direction) introduces a relative phase shift α between the x- and the y-polarization component, giving rise to a rotation of optical quadratures x_L and p_L [Fig. 1(b), (ii)] around the x axis: $x_L \to x_{L,\alpha} = x_L \cos\alpha + p_L \sin\alpha$, $p_L \to p_{L,\alpha} = p_L \cos\alpha - x_L \sin\alpha$. Next, the beam is reflected back into the sample, at a small angle ϕ with respect to the $-z$ direction. In the limit $\phi \to 0$, one approximately obtains the interaction $V_2 = -\frac{\hbar\chi}{\sqrt{T}} J_z p_{L,\alpha}(d_1)$, where the spatial argument reflects the fact that this interaction happens after the pulse has traveled some distance d_1 in the loop between the mirrors and the minus sign stems from the change of the light propagation direction. Then, after passing WP2 (also with its optical axis along the x direction) and traveling a distance d', the third interaction $V_3 = \frac{\hbar\chi}{\sqrt{T}} J_z p_{L,\beta}(d_2)$ happens, where $d_2 = d_1 + d'$ and $\beta = \alpha + \alpha'$, with α' the relative phase shift induced by WP2. Altogether, the triple-pass interaction can be described by $H = H_A + H_L + V_1 + V_2 + V_3$, where $H_A = \hbar\Omega J_x$ refers to the precession of J_y and J_z around the x axis at frequency Ω due to the magnetic field, and H_L denotes the Hamiltonian for the free-space radiation field. From this Hamiltonian, one may evaluate the Heisenberg equations for the light and atoms, yielding the following equations of motion (see Appendix A for details):

$$\frac{d}{dt} J_y(t) = -\Omega J_z(t) + \frac{\chi}{\sqrt{T}} \langle J_x \rangle [p_L(0, t)$$
$$- p_{L,\alpha}(d_1, t) + p_{L,\beta}(d_2, t)], \quad (3)$$

$$\frac{d}{dt} J_z(t) = \Omega J_y(t), \quad (4)$$

$$(\partial_t + c\partial_z) x_L(r, t) = \frac{c\chi}{\sqrt{T}} J_z(t) [\delta(r) - \delta(r - d_1) \cos\alpha.$$
$$+ \delta(r - d_2) \cos\beta], \quad (5)$$

$$(\partial_t + c\partial_z) p_L(r, t) = -\frac{c\chi}{\sqrt{T}} J_z(t) [\delta(r - d_1) \sin\alpha$$
$$+ \delta(r - d_2) \sin\beta], \quad (6)$$

where we have assumed that the spin-light coupling is weak, so that the spin orientation does not deviate much from the x direction during the interaction. Under this assumption one may omit the time evolution of the x component and replace J_x with its average value. Equation (3) has a clear interpretation: At a certain instant in time t, the collective spin J_z simultaneously receives information from three light spatial modes, which reflects the fact that these spatial modes overlap in the cell. To solve the atomic equation, (3), we first solve Eqs. (5) and (6) for the light and then substitute the results into Eq. (3), yielding

$$
\frac{d}{dt} J_y(t) = -\Omega J_z(t) + \frac{\chi^2}{T} \langle J_x \rangle [\sin \alpha J_z(t - d_1/c).
$$
$$
- \sin(\alpha - \beta) J_z(t - d_2/c + d_1/c)
$$
$$
- \sin \beta J_z(t - d_2/c)] + \frac{\chi}{\sqrt{T}} \langle J_x \rangle \mathcal{F}_L(t), \quad (7)
$$

with $\mathcal{F}_L = (1 - \cos \alpha + \cos \beta) p_L(-ct, 0) - (\sin \beta - \sin \alpha) x_L(-ct, 0)$. The terms in square brackets denote the atomic information brought back by light, whose time arguments reflect the time when the collective spin J_z is interacting with the respective light field. The last term in Eq. (7) indicates that the light leaves its information $\mathcal{F}_L$ in the sample, which, as analyzed above, is unwanted for spin squeezing. However, if WP1 and WP2 are both $\lambda/6$ wave plates, we have $\alpha = \pi/3$ and $\beta = 2\pi/3$, which means $\mathcal{F}_L = 0$. This is consistent with the intuitive plots in Fig. 2. Moreover, to further simplify Eq. (7), we make the experimentally feasible assumption that $d_{1,2}/c \ll 1/\Omega$, which means that the elapsed time during the light running in the loop is much shorter than the Larmor period [27]. Under this assumption, we approximately have $J_z(t - d_{1,2}/c) \simeq J_z(t - d_2/c + d_1/c) \simeq J_z(t)$ and, finally, obtain

$$
\frac{d}{dt} \begin{pmatrix} J_y(t) \\ J_z(t) \end{pmatrix} = \begin{pmatrix} 0 & \frac{\sqrt{3}\kappa^2}{2T} - \Omega \\ \Omega & 0 \end{pmatrix} \begin{pmatrix} J_y(t) \\ J_z(t) \end{pmatrix}, \quad (8)
$$

where we have defined the dimensionless coupling constant $\kappa^2 = \chi^2 \langle J_x \rangle = N_{ph} N_{at} (\sigma \Gamma / A \Delta)^2$.

Next, we let $\Omega = \sqrt{3}\kappa^2/4T$, which means that the angular velocity of the transverse spin induced by the magnetic field is the same as the angular velocity caused by the OAT dynamics, but with opposite direction. Under this condition, Eq. (8) can be directly solved to yield

$$
J_{\pi/4}^{out} = e^{\frac{\sqrt{3}\kappa^2}{4}} J_{\pi/4}^{in}, \quad J_{3\pi/4}^{out} = e^{-\frac{\sqrt{3}\kappa^2}{4}} J_{3\pi/4}^{in}, \quad (9)
$$

which represents the main result of this paper. It is evident that a pure TAT transformation $U_{TAT} = e^{-i\sqrt{3}\chi^2(J_y^2 - J_z^2)/8}$ is successfully applied to the spin state. Spin fluctuations are now squeezed along the $\theta = 135°$ direction of the transverse spin at a rate that shrinks them exponentially, yielding the squeezing parameter [Eq. (1)] $\xi^2 = \exp(-\sqrt{3}\kappa^2/2)$. Compared to the DP scheme, whose squeezing parameter is $\xi_{DP}^2 = 1 + (\kappa^4/2 + \kappa^2) [1 - \sqrt{1 + 4/(2 + \kappa^2)^2}] \Rightarrow \lim_{\kappa \to \infty} 2/\kappa^2$ [17], our scheme strongly enhances the degree of squeezing.

V. IMPERFECTIONS

So far, we have neglected the imperfections of the scheme. In deriving Eq. (2), we have assumed $\phi \to 0$ for the angle
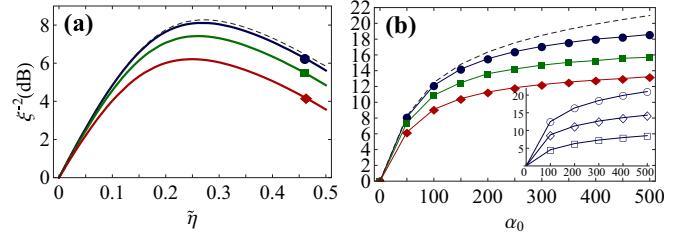

FIG. 3. Calculated squeezing vs photon number (expressed in terms of atomic decay $\tilde{\eta}$) and optical depth α_0, for three values of photon loss. (a) Optimal squeezing ξ^2 vs total photon number for $\phi = 0.05$ and $\alpha_0 = 50$. (b) Peak squeezing vs optical depth α_0. Lines with symbols from top to bottom: no optical loss $\zeta = 0\%$ (blue line with circles), $\zeta = 2\%$ (green line with squares), $\zeta = 6\%$ (brown line with diamonds), and $\phi = 0.05$. Dashed lines denote the case of no optical loss and $\phi = 0$. Inset: Performance of different ideal spin-squeezing protocols versus optical depth, from bottom to top: double pass in [16] (open squares), our OAT (open diamonds), and our TAT (open circles).

between the beams. Although, in principle, the angle ϕ can be made arbitrarily small by, e.g., prolonging the length $d_{1,2}$ of the loop, it remains finite. As a result, the p_L quadrature will see not only the spin J_z, but also J_y during the second and the third passages, which effectively transforms the interaction into $V_2 \to V_2' \propto J_{\pi+\phi} p_{L,\alpha}$, $V_3 \to V_3' \propto J_{2\pi-\phi} p_{L,\beta}$. Also, atomic decay from the weakly populated excited state causes a random rotation of the ground-state spin and shortens the total spin, $\langle J_x \rangle \to \langle J_x \rangle (1 - \tilde{\eta})$, where $\tilde{\eta} \approx 3\eta$, with the factor of 3 originating from the light overlap in the atomic sample and η being proportional to the intensity of the input optical field. We neglect spin decoherence from wall collisions (see the next paragraph). Correspondingly, the transverse spin components now evolve as $\dot{J}_i = i[H, J_i]/\hbar - \tilde{\eta} J_i/2T + \sqrt{\tilde{\eta}/T} f_{J_i}$ with $i \in \{y, z\}$, where f_{J_i} represents the Langevin noise operators with zero mean and $\langle f_{J_i}(t), f_{J_i}(t') \rangle = \langle J_x \rangle \delta(t - t')/2$.

Furthermore, the light is subject to loss. The above decay event acts as a source of absorption or decoherence for light and reduces the probe photons by the factor $\epsilon = N_{at}\eta/N_{ph}$ [28]. Another loss mechanism is reflection off the cell walls due to their finite reflectivity r_0. Leaving and re-entering the cell through one window gives reflectivity $r = 2r_0$. The loss effect can be modeled as a beam-splitter-type admixture of vacuum components, which transforms the quadratures at $r = d_n$ ($n = 1, 2$) into $q(d_n) \to \sqrt{1 - n\zeta} q(d_n) + \sqrt{n\zeta} f_{Lq,3n}$ [29], where $\zeta = \epsilon + 2r_0$ denotes the overall loss rate caused by crossing the sample through two cell walls, and $f_{Lq,3n} = \sum_{i=1}^{3n} f_{Lq}^i/\sqrt{3n}$ represents the vacuum noise operator, with f_{Lq}^i the Langevin operator of light admixed during the ith crossing.

After considering all the above imperfections (see Appendix B for details) and optimizing the protocol with respect to the magnetic field and the relative phases introduced by the wave plates, we obtain curves showing (Fig. 3) the squeezing ξ^2 vs the photon number (drawn as the decay parameter $\tilde{\eta}$) for different photon losses, with $\phi = 0.05$ and the optical depth $\alpha_0 = 50$. As shown, for each photon loss ζ, there exists a maximal squeezing, achieved at a certain photon number ($\propto \tilde{\eta}$). Strong squeezing of more than 7.4 dB
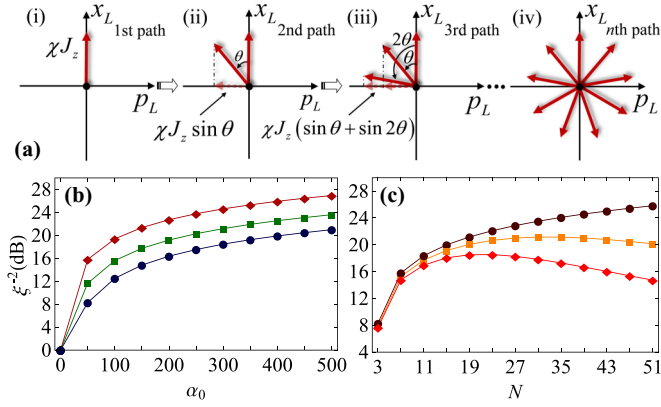
FIG. 4. (a) Phase-space portrait of the light's noise evolution induced by the multipass scheme (we here depict the nine-pass as an example). During the first path, atomic noise J_z is mapped onto x_L ($\propto S_y$). (ii) After a polarization rotation by an angle $2\pi/N$ produced by a wave plate, the second path imprints the atomic noise J_z onto the x_L quadrature. (iii) After another $2\pi/N$ rotation by the wave plate, x_L "sees" J_z again. After the $(N-1)$th rotation by the wave plate and the Nth path, we finally arrive at (iv). The sum of the N spin contribution is 0 to ensure the cancellation of the spin-probe entanglement. Dashed red arrows along the x_L axis are the atomic information brought back by light in each path. (b) For the case of TAT, the dependence of the squeezing ξ^2 on the optical depth α_0 for different numbers of passes N, with $N = 7$, 4, and 3, from top to bottom. (c) Dependence of squeezing on the number of passes N, for $\alpha_0 = 50$, with optical loss of 0, 0.5%, and 1% per pass, from top to bottom. We assume $\phi = 0$ in both (b) and (c).

is achievable for $\zeta = 2\%$. For $\zeta = 6\%$, a very respectable squeezing of 6.2 dB is still seen. The peak squeezing as a function of α_0 for different light losses is plotted in Fig. 2(b). For an atomic system with the large OD of $\alpha_0 = 100$, the degree of squeezing created should be as high as 10.9 dB for $\zeta = 2\%$. A comparison of the performances of different protocols [inset in Fig. 3(b)] shows that our schemes greatly enhance the amount of achievable squeezing. The increase in squeezing compared to that in the scheme without quantum erasure [16] is about 10 dB for an OD of 500.

VI. GENERALIZATION TO MULTIPASS QUANTUM ERASURE

We found that, to realize the above unitary OAT and TAT spin squeezing, the number of passes through the atomic medium does not have to be three. In fact, we can generalize the current three-pass scheme to an N-pass ($N \geqslant 3$) scheme. To illustrate how this works, we again use the phase-space portrait of the light's noise evolution as shown in Fig. 4(a). For simpler illustration, we assume that the point in the phase space for light initially is at the origin of the $x_L p_L$ plane. Furthermore, we assume that, during each interaction, x_L ($\propto S_y$) picks up only the atomic $+J_z$ contribution, which can be realized by using an optical-ring-cavity-like configuration where all the N light passes go through the atomic medium along the same direction. As shown in Fig. 4(a), in each path the probe light picks up information about J_z, which is proportional to the coupling constant χ. Similarly to the three-pass scheme above, the sum of the spin contribution from the N-pass interaction

should be 0 to erase the spin-probe entanglement [see Fig. 4(a), (iv)], which requires a rotation of the Stokes vector around the x axis by an angle $\theta = 2\pi/N$ after each path. From the point of view of the atoms, after the first path the atoms start to receive information about the S_z ($\propto p_L$) of the light in the amount F_i for the ith path, where S_z in each pass is the projection of all the vectors (denoted by red arrows) onto the p_L axis. For instance, for the second pass, the atoms obtain the S_z contribution $F_2 = \chi^2 J_z \sin\theta$ [see Fig. 4(a), (ii)], and for the third pass, $F_3 = \chi^2 J_z(\sin\theta + \sin 2\theta)$. Finally, for the Nth path, we have $F_N = \chi^2 J_z(\sin\theta + \sin 2\theta + \ldots + \sin[(N-1)\theta])$. After all the passes, the atomic spin obtains the information

$$\Lambda = \sum_{i=2}^{N} F_i = \chi^2 J_z \sum_{n=1}^{N-1} (N-n)\sin(n\theta)$$

$$= \frac{N}{2}\cot\left(\frac{\pi}{N}\right)\chi^2 J_z. \tag{10}$$

Apparently, for $N = 3$, the atomic information accumulated is $\Lambda = \sqrt{3}\chi^2 J_z/2$, which agrees with the result derived above. For large N, we have $\Lambda \simeq N^2 \chi^2 J_z/\pi \propto N^2 \alpha_0$, where the enhancement factor of N^2 on the coupling coefficient χ^2 will be reduced to N after we take into account the decay of the collective spin due to spontaneously emitted light or optical loss from the optical windows or mirrors. We found that for large N, the squeezing factor is $\xi^2 \propto 1/(N\alpha_0)$.

We have carried out numerical calculations for different numbers of round trips in the presence of atomic spin loss and optical loss. In Fig. 4(b), we show in the TAT case the squeezing factor ξ^2 vs the optical depth α_0 for three numbers of total passes, $N = 3$, 4, and 7, respectively. Here, the atomic spin loss has been considered, but the optical loss and the angle between the beam passes have been neglected, and we have optimized the laser power for each calculated data point. As can be seen, with the increase in N, the amount of attainable squeezing is significantly improved. In Fig. 4(c), the dependence of squeezing ξ^2 on N is shown for a relatively low OD, $\alpha_0 = 50$, for different values of optical loss and with spin loss taken into account. The laser power has also been optimized for each data point. It is shown that when the optical loss is 0 (upper curve), ξ^2 scales linearly with N for large N. With finite mirror loss, there is an optimal value for N and it increases when the optical loss decreases. Therefore, the multipass approach provides a possible way to realize ultrastrong spin squeezing in low-optical-depth systems, such as room-temperature vapor cells. Furthermore, this multipass scheme should be extendable to an optical ring cavity system, where a cavity birefringence can be introduced to play the role of the wave plates here, and the amount of birefringence can be optimized according to the cavity loss to allow many successive sets of the N-pass quantum erasure described here, but with descending laser power.

VII. EXPERIMENTAL FEASIBILITY OF THE THREE-PASS SCHEME

Our TAT scheme can be implemented in both cold-atom and room-temperature atomic vapor cell systems. Here, we take the latter as an example. Consider a paraffin-coated glass cell filled with warm ^{87}Rb atomic vapor. First, two circularly polarized

beams, which are resonant with the $5S_{1/2}$, $F = 2 \rightarrow 5P_{1/2}$ and $5S_{1/2}$, $F = 1 \rightarrow 5P_{3/2}$ transitions, are sent through the sample along the x direction to pump nearly all the atoms to the ground hyperfine state $|F = 2, m_F = 2\rangle$ forming the coherent spin state. Next, a probe pulse tuned to the D2 line ($\Gamma = 3.03$ MHz) at the large blue detuning of around $\Delta = 1$ GHz is turned on. The probe now couples all five ground states $|m_F = 0, \pm 1, \pm 2\rangle$, which leads to the effective Hamiltonian [30], $H_{\text{eff}} \propto a_1(\Delta)J_z S_z + a_2(\Delta)(\phi_0 J_z^2 - S_- J_+^2 - S_+ J_-^2)$ with $J_\pm = J_x \pm i J_y$ and $S_\pm = S_x \pm i S_y$, where ϕ_0 is the photon density, and a_1 and a_2 are the dimensionless atomic vector and tensor polarizabilities [2,26]. The second term proportional to a_2 is the higher-order couplings between the probe and the atoms. For large detunings, the vector polarizability $a_1(\Delta) \rightarrow 1/24$ and the tensor polarizability $a_2(\Delta) \rightarrow 0$. Then we can neglect the tensor polarizability and keep only the Faraday-type interaction. For a cylindrical cell of diameter 2.5 cm and length 2.5 cm containing 2.0×10^{12} atoms (corresponding to the Heisenberg limit, 120 dB) at temperature $T = 325$ K (atomic density 1.7×10^{11} cm^{-3}), a resonant optical depth $\alpha_0 = 50$ can be achieved. For optimal squeezing, the decay parameter $\tilde{\eta}$ should be within the range 0.10–0.30, corresponding to a photon number per pulse of the order of 10^{14}, with a duration of about 5 ms (spin decoherence by the wall is negligible since the typical T_2 time is more than 100 ms) at the power of 5 mW. Under these conditions, the photon loss ϵ due to atom scattering is less than 2.0×10^{-3} and can be safely neglected. Meanwhile, under the same condition, $\phi = 0.05$, as in the previous section, the distinguishability ϱ (see Appendix C for more detail) is around 1.6×10^{-2}, which sets a limit to the maximal achievable squeezing of 18 dB. Since the typical amount of squeezing for α_0 around 50 (see Fig. 3) is far less than 18 dB, we conclude that imperfect overlap between the beams does not substantially limit the efficiency of the scheme and can be ignored. For a moderate reflectivity, $r_0 = 1\%$ [31], peak squeezing of 7.4 dB is obtained at $\tilde{\eta} = 0.26$, corresponding to the coupling constant $\kappa = 2.08$. The magnetic field added should satisfy $B = \sqrt{3}\hbar\kappa^2/(4g_F\mu_B T)$, with g_F the hyperfine Landé g factor and μ_B the Bohr magneton. For the typical duration of 5 ms, the magnetic field needed is about 0.38 mG, corresponding to a Larmor frequency of 270 Hz. Finally, we note that, although the overlapping laser beams can form a standing wave and introduce an inhomogeneous laser intensity distribution within the atomic sample, it can be averaged out by atomic motion for warm atoms, and in cold atoms it can be eliminated by offsetting the frequency of the three beams to form a moving standing wave.

VIII. CONCLUSION

One additional benefit of our TAT scheme is the existence of the magnetic field. In most spin-squeezing experiments, a magnetic field is added for spin noise detection at the Larmor frequency to avoid technical noise near dc; however, the resulting back-action diminishes the squeezing and needs to be eliminated with complicated experimental configurations [2,32]. Here, since the magnetic-field-induced Larmor precession is built into the scheme, there is simply no back-action. The squeezing process can be understood as a continuous swapping of spin-light entanglement created by the Faraday interactions into spin-spin entanglement. Another intriguing feature of the current TAT method is that it relies on the "simultaneous passage" mechanism, which removes the impractical requirement of long delay lines between passages [33] and greatly simplifies the experiment.

In summary, we have presented a novel scheme for quantum erasure which enables unitary spin squeezing. Schemes for realizing both one-axis- and two-axis-twisting spin squeezing of an atomic ensemble are presented. Under Faraday-type interactions, pure SSSs can be created by simply passing an optical pulse through the Larmor precessing spins three or more times. Neither projective measurements nor feedback control is required. Taking into account the noise effects imposed by several incoherent processes, our calculation shows that substantial squeezing is still obtainable under moderate experimental conditions. This proposal points to new approaches to quantum erasure and unitary spin squeezing and, thus, will advance technologies for quantum metrology and quantum information processing.

APPENDIX A: ATOM-LIGHT INTERACTIONS AND EVOLUTION OF THE SPIN STATE

1. Atom-light interactions

In this Appendix, we present a simple derivation of the Faraday-type Hamiltonian (2), for a two-level system. A more detailed derivation of the effective Hamiltonian for full multilevel coupling can be found in [2] and [26]. The Faraday-type interaction relies on off-resonant coupling between light and an atomic sample, as shown in Fig. 5. The incident light is an x-polarization mode in a strong coherent state, with central frequency ω_c and a narrow bandwidth b. The scattered light propagating in the forward direction is collectively
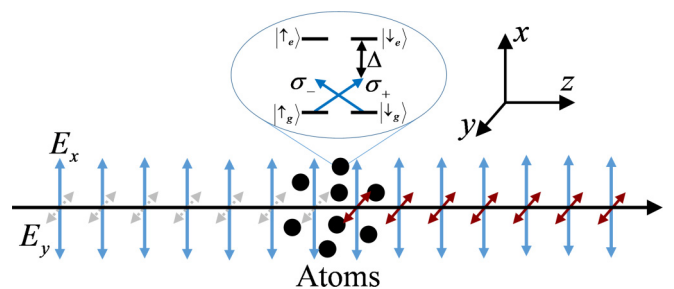

FIG. 5. A coherent pulse propagating in the z direction interacts off-resonantly with an ensemble of atoms with ground states $|\uparrow_g\rangle, |\downarrow_g\rangle$ and excited states $|\uparrow_e\rangle, |\downarrow_e\rangle$. The x polarization of the pulse is in a strong coherent state (blue arrow) and the y polarization is in the vacuum state (gray arrow). The forward-scattered light is in the y polarization and also propagates along z (red arrow).

enhanced [34], which is in y-polarization mode and is relevant here, while light scattering in other directions is treated as noise. Here, for simplicity, we consider a single-mode light with wave number k interacting with a cloud of atoms with the relevant level structure shown in Fig. 5. In a frame rotating at the frequency $\omega_k = kc$ of light, the interaction Hamiltonian is given by

$$H = \sum_{l=1}^{N_{\text{at}}} [\hbar g_k (a_{k,+} |\downarrow_{e,l}\rangle\langle\uparrow_{g,l}| + a_{k,-}|\uparrow_{e,l}\rangle\langle\downarrow_{g,l}| + \text{H.c.})$$
$$+ \hbar \Delta_k (|\uparrow_{e,l}\rangle\langle\uparrow_{e,l}| + |\downarrow_{e,l}\rangle\langle\downarrow_{e,l}|)], \qquad (A1)$$

where g_k is the coupling strength, $a_{k,+} = (-a_{k,x} + i a_{k,y})/\sqrt{2}$ and $a_{k,-} = (a_{k,x} + i a_{k,y})/\sqrt{2}$ denote the annihilation operators of right and left circularly polarized light modes, respectively, and $\Delta_k = \omega_{\text{at}} - \omega_k$ is the detuning. For large detuning $\Delta_k \gg g$, we can adiabatically eliminate the excited states $|\uparrow_e\rangle, |\downarrow_e\rangle$ and obtain the effective Hamiltonian

$$H_{\text{eff}} = -\frac{\hbar g_k^2}{\Delta_k} \sum_{l=1}^{N_{\text{at}}} (|\uparrow_{g,l}\rangle\langle\uparrow_{g,l}|a_{k,+}^\dagger a_{k,+} + |\downarrow_{g,l}\rangle\langle\downarrow_{g,l}|a_{k,-}^\dagger a_{k,-}).$$
$$(A2)$$

Equation (A2) indicates that the influence of the light mode on the spins can be understood as the ac Stark shift induced by the imbalance between σ_+ and σ_- components, which thus changes the relative phase between $|\uparrow_g\rangle$ and $|\downarrow_g\rangle$. In turn, the slight population differences between $|\uparrow_g\rangle$ and $|\downarrow_g\rangle$ cause a tiny rotation of the linear polarization, known as the Faraday effect. Using the relation between linear and circular annihilation operators, Eq. (A2) can be reexpressed as

$$H_{\text{eff}} = -\frac{\hbar g_k^2}{\Delta_k} \left[N_{\text{at}} N_{\text{ph}}^k - \frac{1}{2i}(a_{k,x}^\dagger a_{k,y} - a_{k,y}^\dagger a_{k,x}) \right.$$
$$\left. \times \sum_{l=1}^{N_{\text{at}}} (|\downarrow_{g,l}\rangle\langle\downarrow_{g,l}| - |\uparrow_{g,l}\rangle\langle\uparrow_{g,l}|) \right], \qquad (A3)$$

where $N_{\text{ph}}^k = a_{k,x}^\dagger a_{k,x} + a_{k,y}^\dagger a_{k,y}$ is the number of photons. The first term in (A3) gives rise to an overall Stark shift of the ground states and can thus be ignored. We now introduce the definition of Stokes operators for light $S_{k,x} = (a_{k,x}^\dagger a_{k,x} - a_{k,y}^\dagger a_{k,y})/2$, $S_{k,y} = (a_{k,x}^\dagger a_{k,y} + a_{k,y}^\dagger a_{k,x})/2$, and $S_{k,z} = (a_{k,x}^\dagger a_{k,y} - a_{k,y}^\dagger a_{k,x})/2i$, satisfying the angular momentum-type commutation relations $[S_{k,y}, S_{k,z}] = i S_{k,x}$. By use of the spin definition for collective atoms $J_z = \frac{1}{2}\sum_{l=1}^{N_{\text{at}}} (|\downarrow_{g,l}\rangle\langle\downarrow_{g,l}| - |\uparrow_{g,l}\rangle\langle\uparrow_{g,l}|)$, the Hamiltonian takes the form $H_{\text{eff}} = \frac{2\hbar g_k^2}{\Delta_k} J_z S_{k,z}$. Since the x-polarized mode is in a strong coherent state, we can replace $a_{k,x}$ with its expectation value $\langle a_{k,x}\rangle$ and get $H_{\text{eff}} \propto -i(a_{k,y} - a_{k,y}^\dagger)J_z/\sqrt{2} = p_{k,L} J_z$. By taking into account all of the light modes in the narrow bandwidths b [34], one will finally arrive at Hamiltonian (2).

It is noteworthy that, for the Hamiltonian we consider here, it is the intensity of the light that affects the phase of the atomic spin through the ac Stark shift, and the phase of the light does not enter directly. This is different from many quantum memory protocols where the phase of the light is mapped onto the atomic spin. This fact helps to simplify the analysis of the effects of nonoverlapping beams in the following sections.

2. Evolution of the spin state

According to the Hamiltonian H given in the text, one may evaluate the Heisenberg equations $\partial_t \mathbf{J} = \frac{1}{i\hbar}[\mathbf{J}, H]$ for atoms and the Maxwell-Bloch equations $(\partial_t + c\partial_z)q(z,t) = \frac{1}{i\hbar}[q(z,t), H]$ for light [26], yielding

$$\frac{d}{dt} J_x(t) = -\frac{\chi}{\sqrt{T}} J_y [p_{L}(0,t) - p_{L,\alpha}(d_1,t) + p_{L,\beta}(d_2,t)], \qquad (A4)$$

$$\frac{d}{dt} J_y(t) = -\Omega J_z(t) + \frac{\chi}{\sqrt{T}} J_x [p_L(0,t) - p_{L,\alpha}(d_1,t) + p_{L,\beta}(d_2,t)], \qquad (A5)$$

$$\frac{d}{dt} J_z(t) = \Omega J_y(t), \qquad (A6)$$

$$(\partial_t + c\partial_z)x_L(r,t) = \frac{c\chi}{\sqrt{T}} J_z(t)[\delta(r) - \delta(r - d_1)\cos\alpha + \delta(r - d_2)\cos\beta], \qquad (A7)$$

$$(\partial_t + c\partial_z)p_L(r,t) = -\frac{c\chi}{\sqrt{T}} J_z(t)[\delta(r - d_1)\sin\alpha - \delta(r - d_2)\sin\beta]. \qquad (A8)$$

The first terms in (A5) and (A6) describe the Larmor precession of the atomic system around the x axis, while the first term in (A4) and the second term in (A5) describe the rotation of the collective spin around the z axis caused by the three successive light passes through the atomic ensemble. To simplify this set of coupled equations, we make the experimentally reasonable assumption that the spin-light coupling is weak, so that the light-induced rotation of the collective spin is small. Under this assumption, one may neglect the deviation of the macroscopic component J_x from the x direction after the interaction [Eq. (A4) can therefore be omitted] and treat the operator J_x with a c number, $J_x \approx \langle J_x\rangle$. Next, we introduce a new position variable, $\tilde{r} = ct - r$, which represents a coordinate system fixed on the light pulse and allows us to denote particular pieces of the propagating pulse easily [2,26]. By this definition, the above equations become

$$\frac{d}{dt} J_y(t) = -\Omega J_z(t) + \frac{\chi}{\sqrt{T}} \langle J_x\rangle [\bar{p}_{L}(ct,t) - \bar{p}_{L,\alpha}(ct - d_1,t) + \bar{p}_{L,\beta}(ct - d_2,t)], \qquad (A9)$$

$$\frac{d}{dt} J_z(t) = \Omega J_y(t), \qquad (A10)$$

$$\partial_t \bar{x}_L(\tilde{r},t) = \frac{c\chi}{\sqrt{T}} J_z(t)[\delta(ct - \tilde{r}) - \delta(ct - \tilde{r} - d_1)\cos\alpha + \delta(ct - \tilde{r} - d_2)\cos\beta], \qquad (A11)$$

$$\partial_t \bar{p}_L(\tilde{r},t) = -\frac{c\chi}{\sqrt{T}} J_z(t)[\delta(ct - \tilde{r} - d_1)\sin\alpha - \delta(ct - \tilde{r} - d_2)\sin\beta], \qquad (A12)$$

where we have defined the new light quadratures $\bar{q}_L(\tilde{r},t) = \bar{q}_L(ct - \tilde{r},t)$. To solve the equations for atoms, one must first solve the equations for light. By integrating Eqs. (A11) and (A12) over t on both sides, the Dirac delta functions are

then turned into the Heaviside step functions $\Theta(\cdot)$:

$$
\begin{aligned}
\bar{x}_L(\tilde{r},t) = {}& \bar{x}_L(\tilde{r},0) + \frac{\chi}{\sqrt{T}}[J_z(\tilde{r}/c)\Theta(t - \tilde{r}/c) \\
& - J_z(\tilde{r}/c + d_1/c)\Theta(t - \tilde{r}/c - d_1/c)\cos\alpha \\
& + J_z(\tilde{r}/c + d_2/c)\Theta(t - \tilde{r}/c - d_2/c)\cos\beta],
\end{aligned}
$$

$$
\begin{aligned}
\bar{p}_L(\tilde{r},t) = {}& \bar{p}_L(\tilde{r},0) - \frac{\chi}{\sqrt{T}}[J_z(\tilde{r}/c + d_1/c) \\
& \Theta(t - \tilde{r}/c - d_1/c)\sin\alpha - J_z(\tilde{r}/c + d_2/c) \\
& \Theta(t - \tilde{r}/c - d_2/c)\sin\beta].
\end{aligned}
$$

The light quadratures $\bar{p}_L(ct,t)$, $\bar{p}_{L,\alpha}(ct - d_1,t)$, $\bar{p}_{L,\beta}(ct - d_2,t)$ in Eq. (A9) can then be calculated to give, respectively,

$$
\bar{p}_L(ct,t) = \bar{p}_L(ct,0), \tag{A13a}
$$

$$
\begin{aligned}
\bar{p}_{L,\alpha}(ct - d_1,t) = {}& \bar{p}_{L,\alpha}(ct - d_1,0) \\
& - \frac{\chi}{\sqrt{T}}J_z(t - d_1/c)\sin\alpha, \tag{A13b}
\end{aligned}
$$

$$
\begin{aligned}
\bar{p}_{L,\beta}(ct - d_2,t) = {}& \bar{p}_{L,\beta}(ct - d_2,0) \\
& - \frac{\chi}{\sqrt{T}}[J_z(t - d_2/c)\sin\beta \\
& + J_z(t - d_2/c + d_1/c)\sin(\alpha - \beta)]. \tag{A13c}
\end{aligned}
$$

Obviously, these three-momentum quadratures are simultaneously 'seen' by the spin component J_z. At time $t = t$, the piece $\tilde{r} = ct$ of the pulse enters the atomic sample for the first time, therefore it contains, as can be seen in Eq. (A13a), no information about atoms. The situation for the piece $\xi = ct - d_1$, however, is different. Since it sits in front of $\xi = ct$ at a distance d_1, information on J_z was marked on $\bar{p}_{L,\alpha}(ct - d_1)$ at an earlier time c/d_1 [see Eq. (A13b)]. The piece $\tilde{r} = ct - d_2$ carries information about J_z at different times [the two terms in square brackets in Eq. (A13c)], which was picked up by this piece of light during its first and second interactions with the atoms. Substituting (A13) into (A9), one

obtains

$$
\begin{aligned}
\frac{d}{dt}J_y(t) = {}& -\Omega J_z(t) + \frac{\chi^2}{T}\langle J_x\rangle[J_z(t - d_1/c)\sin\alpha \\
& - J_z(t - d_2/c)\sin\beta \\
& - J_z(t - d_2/c + d_1/c)\sin(\alpha - \beta)] \\
& + \frac{\chi}{\sqrt{T}}\langle J_x\rangle[\bar{p}_L(ct,0) - \bar{p}_{L,\alpha}(ct - d_1,0) \\
& + \bar{p}_{L,\beta}(ct - d_2,0)]. \tag{A14}
\end{aligned}
$$

Note that, in reality, the distances $d_{1,2}$ along the optical path are usually of the order of meters, which is much shorter than the spatial extension of the spatially localized light modes, that is, c/b (where b is assumed to be of the order of megahertz). We therefore can neglect the spatial arguments of the light operators in (A14) and, finally, arrive at Eq. (7) in the text.

APPENDIX B: IMPERFECTION OF THE SCHEME

So far, we have neglected the imperfections of the setup as well as the noise effects. In deriving Eq. (2), we have used the condition $\phi \to 0$, while in reality the angle ϕ is a small but nonzero parameter, which transforms the total Hamiltonian into

$$
\begin{aligned}
H = {}& \hbar\Omega J_x + \frac{\hbar\chi}{\sqrt{T}}[J_z p_L(0) + J_{\pi+\phi}p_{L,\alpha}(d_1) \\
& + J_{2\pi-\phi}p_{L,\beta}(d_2)]. \tag{B1}
\end{aligned}
$$

As for noise effects, as mentioned in the text, on the one hand, atoms undergo dissipation due to collisional relaxation and weak excitation by the probe light, which causes decoherence of the transverse components of the spin state at a rate of $\tilde{\eta}/T$. On the other hand, light also suffers losses due to reflections by the cell walls and incoherent scattering by atoms. Such losses, affecting both the quantum variables and the classical field, can be characterized by the reflection coefficient ζ.

By taking into account the effect of the small angle ϕ and the atomic damping, the atomic evolution equations (A9) and (A10), are changed into

$$
\frac{d}{dt}J_y(t) = -\Omega J_z(t) - \frac{\tilde{\eta}}{2T}J_y(t) + \frac{\chi}{\sqrt{T}}\langle J_x\rangle[\bar{p}_L(ct,t) - \sqrt{1-\zeta}\,\bar{p}_{L,\alpha}(ct - d_1,t)\cos\phi + \sqrt{1-2\zeta}\,\bar{p}_{L,\beta}(ct - d_2,t)\cos\phi] + \sqrt{\frac{\tilde{\eta}}{T}}f_{J_y}, \tag{B2}
$$

$$
\frac{d}{dt}J_z(t) = \Omega J_y(t) - \frac{\tilde{\eta}}{2T}J_z(t) - \frac{\chi}{\sqrt{T}}\langle J_x\rangle[\sqrt{1-\zeta}\,\bar{p}_{L,\alpha}(ct - d_1,t) + \sqrt{1-2\zeta}\,\bar{p}_{L,\beta}(ct - d_2,t)]\sin\phi + \sqrt{\frac{\tilde{\eta}}{T}}f_{J_z}. \tag{B3}
$$

Each time the pulse transits through the ensemble, photon scattering losses occurs. Before the next transit of the pulse through the atoms, it must cross two cell walls, which introduces photon reflection losses. These losses lead to a decrease in the total photon number N_{ph} and, thus, reduce the coupling strength in terms of $\chi \to \sqrt{1 - (n-1)\zeta}\,\chi$, where n accounts for the nth interaction of light with atoms. Here, we have neglected the light reflection by the first wall. Since the input light state involved here is a coherent state, the losses due to the first crossing can always be compensated by using a more intense pulse [35]. The loss process also affects the quantum variables and transforms (according to the text) the light quadratures of (A13) into

$$
\bar{p}_L(ct,t) = \bar{p}_L(ct,0), \tag{B4a}
$$

$$
\bar{p}_{L,\alpha}(ct - d_1,t) = \sqrt{1-\zeta}\left[\bar{p}_{L,\alpha}(ct - d_1,0) - \frac{\chi}{\sqrt{T}}J_z(t - d_1/c)\sin\alpha\right] + \sqrt{\zeta}\,F_{L\alpha,3}(t), \tag{B4b}
$$

$$
\bar{p}_{L,\beta}(ct - d_2,t) = \sqrt{1-2\zeta}\left\{\bar{p}_{L,\beta}(ct - d_2,0) - \frac{\chi}{\sqrt{T}}[J_z(t - d_2/c)\sin\beta - J_{\pi+\phi}(t - d_2/c + d_1/c)\sin(\alpha - \beta)]\right\} + \sqrt{2\zeta}\,F_{L\beta,6}(t), \tag{B4c}
$$

where we have defined the collective light noise operators $F_{L\vartheta,m} = f_{Lp,m}\cos\vartheta - f_{Lx,m}\sin\vartheta$. By inserting Eqs. (B4) into (B3) and (B4), one may obtain the new evolutions for atoms:

$$\partial_t\begin{pmatrix} J_y(t) \\ J_z(t) \end{pmatrix} = C_1\begin{pmatrix} J_y(t) \\ J_z(t) \end{pmatrix} + C_2\begin{pmatrix} \bar{x}_L(ct,0) \\ \bar{p}_L(ct,0) \end{pmatrix} + C_3\begin{pmatrix} F_{L\alpha,3}(t) \\ F_{L\beta,6}(t) \end{pmatrix} + \sqrt{\frac{\eta}{T}}\begin{pmatrix} f_{J_y}(t) \\ f_{J_z}(t) \end{pmatrix}. \tag{B5}$$

Here the coefficients matrix C_1, C_2, and C_3 can easily be calculated to give

$$C_1 = -\frac{1}{T}\begin{pmatrix} \frac{\tilde{\eta}}{2} - \frac{\kappa^2}{2}(1-2\zeta)\sin 2\phi\sin(\alpha-\beta) & \Omega T - \cos\phi\kappa^2[S_- - (1-2\zeta)\cos\phi\sin(\alpha-\beta)] \\ -\Omega T + \kappa^2(1-2\zeta)\sin\phi^2\sin(\alpha-\beta) & \frac{\tilde{\eta}}{2} - \sin\phi\kappa^2[S_+ + (1-2\zeta)\cos\phi\sin(\alpha-\beta)] \end{pmatrix}, \tag{B6}$$

$$C_2 = -\frac{\chi}{\sqrt{T}}\langle J_x\rangle\begin{pmatrix} -\cos\phi S_- & -1+\cos\phi C_- \\ \sin\phi S_+ & \sin\phi C_+ \end{pmatrix}, \tag{B7}$$

$$C_3 = -\frac{\chi}{\sqrt{T}}\langle J_x\rangle\begin{pmatrix} \cos\phi\sqrt{(1-\zeta)\zeta} & -\cos\phi\sqrt{(1-2\zeta)2\zeta} \\ \sin\phi\sqrt{(1-\zeta)\zeta} & \sin\phi\sqrt{(1-2\zeta)2\zeta} \end{pmatrix}, \tag{B8}$$

with $S_\pm = (1-\zeta)\sin\alpha \pm (1-2\zeta)\sin\beta$, $C_\pm = (1-\zeta)\cos\alpha \pm (1-2\zeta)\cos\beta$. Equation (B5) can then be directly solved to yield the input-output relation for the atoms,

$$\begin{pmatrix} J_y^{\text{out}} \\ J_z^{\text{out}} \end{pmatrix} = C(T)\begin{pmatrix} J_y^{\text{in}} \\ J_z^{\text{in}} \end{pmatrix} + C(T)\int_0^T d\tau\, C^{-1}(\tau)\left[C_2\begin{pmatrix} \bar{x}_L(c\tau,0) \\ \bar{p}_L(c\tau,0) \end{pmatrix} + C_3\begin{pmatrix} F_{L\alpha,3}(\tau) \\ F_{L\beta,6}(\tau) \end{pmatrix} + \sqrt{\frac{\eta}{T}}\begin{pmatrix} f_{J_y}(\tau) \\ f_{J_z}(\tau) \end{pmatrix}\right], \tag{B9}$$

where $C(t) = e^{C_1 t}$. Note that, unlike the ideal case, now the light quadratures in (B9) cannot freely be canceled, since the adjustment of the phase shifts α and β, on the other hand, will amplify the noise effects of the light. As a result, there exists an optimal choice of α and β, with which the amount of squeezing can be maximized.

APPENDIX C: EFFECTS OF NONOVERLAPPING OF LIGHT BEAMS

In the above derivation, we have assumed that the light beam interacts with the same collective spin during each pass, while in reality, in order to remove the light beam from the sample in the third pass, the three spatial light modes should not be completely overlapping, which leads to slightly different collective-spin light couplings in each path. In other words, the macroscopic spins seen by the beams in the three passes would be slightly different. We here evaluate the effects of nonoverlapping of light beams and evaluate its influence on the unitary OAT scheme.

First, for simplicity, we neglect all the losses and assume that the light beam in the first pass covers the entire sample, which leads to the interaction $V_1 \propto J_z p_L$. For the second and third interactions, because of the deviation of the light propagating direction along z by an angle ϕ, the beams see only part of the collective spin. The atoms in the sample can be classified into three categories as follows: (i) Most atoms see all three beams, forming a subcollective spin J_{I} (the common spin mode). (ii) Some atoms can only see the beams in the first and second passes, described by the collective spin J_{II}. (iii) J_{III} denotes the collective spin seen by the beam only during the first and third passes. By these definitions, the second and third interactions are described by $V_2 \propto (J_{\text{I},z} + J_{\text{II},z})p_{L,\pi/3}$ and $V_3 \propto (J_{\text{I},z} + J_{\text{III},z})p_{L,2\pi/3}$, respectively, where we have assumed $\phi \ll 1$ and therefore neglected those terms proportional to ϕ, for simplicity. Note that here we have the relation $J_z = J_{\text{I},z} + J_{\text{II},z} + J_{\text{III},z}$. To model the continuous interaction between the moving atoms

and the light field, we can mathematically split the light pulse into independent slices of duration $\tau_0 = T/m$ (m is an integer) and first consider the time evolution of the atomic sample during this interval. If τ_0 is small enough, the sample can be treated as motionless atoms. During this interval, one can derive the input-output relations for atoms according to the Hamiltonian outlined above:

$$J_z^{\text{out}} = J_z^{\text{in}},$$
$$J_y^{\text{out}} = J_y^{\text{in}} + \frac{1}{2}\frac{\chi}{\sqrt{m}}(\langle J_{\text{III},x}\rangle + \langle J_{\text{II},x}\rangle)p_L^{\text{in}}$$
$$+ \frac{\sqrt{3}}{2}\frac{\chi}{\sqrt{m}}(\langle J_{\text{III},x}\rangle - \langle J_{\text{II},x}\rangle)(x_L^{\text{in}} + \chi J_z^{\text{in}})$$
$$+ \frac{\sqrt{3}}{2}\frac{\chi^2}{m}(\langle J_{\text{III},x}\rangle + \langle J_{\text{I},x}\rangle)(J_{I,z}^{\text{in}} + J_{II,z}^{\text{in}}). \tag{C1}$$

For a symmetrical setup of the light path which is assumed here, it is reasonable to assume $\langle J_{\text{III},x}\rangle = \langle J_{\text{II},x}\rangle$. We then define the new parameter $\varrho \ll 1$, which describes the distinguishability of the light modes such that $\langle J_{\text{II},x}\rangle = \langle J_{\text{III},x}\rangle = \varrho\langle J_{\text{I},x}\rangle$ (the larger the ϱ, the more distinguishable the three light modes). Equation (C1) is then reduced to

$$J_z^{\text{out}} = J_z^{\text{in}},$$
$$J_y^{\text{out}} = J_y^{\text{in}} + \varrho\frac{\chi}{\sqrt{m}}\langle J_{\text{I},x}\rangle p_L^{\text{in}}$$
$$+ (1+\varrho)\frac{\sqrt{3}}{2m}\chi^2\langle J_{\text{I},x}\rangle(J_{\text{I},z}^{\text{in}} + J_{\text{II},z}^{\text{in}}). \tag{C2}$$

Equation (C2) indicates that (i) there is residual entanglement between light and atoms which is proportional to the number of atoms out of the common spin mode J_{I}, and (ii) the spin-spin entanglement induced by the OAT nonlinearity only appears among those atoms covered by the beam in the second pass (already in the first-pass beam), which we call the interaction region (IR). From Eq. (C2) one can calculate the amount of

squeezing,

$$\xi^2 = 1 + \frac{(1+\varrho)\tilde{\kappa}^2}{2(1+2\varrho)}(\tilde{\kappa}^2 + c^2)\left(1 - \sqrt{1 + \frac{4}{(\tilde{\kappa}^2 + c^2)^2}}\right), \quad \text{(C3)}$$

where we have defined $\tilde{\kappa}^2 = \frac{\sqrt{3}}{2m}(1+\varrho)\kappa^2$ and $c^2 = \frac{2\varrho^2}{\sqrt{3}(1+\varrho)^2}$. For a cold sample, atoms remain almost still during the time of interactions, and thus, after the mth interaction, the squeezing parameter for a high coupling strength and small ϱ can be approximately expressed as $\xi^2 \approx \frac{4}{3\kappa^4} + \frac{4}{3\kappa^2}\varrho^2 + \varrho$, where the first term stems from the unitary OAT evolution contributed by J_{I}, the second term arises because of the atom-light entanglement from J_{II}, and the last term comes from the shot noise contributed by atoms out of the IR (J_{III}). We note that when the spin loss is considered, the κ^4 scaling of the first term reduces to $\kappa^{4/3}$, and the κ^2 scaling of the second term reduces to $\kappa^{3/5}$ [17]. The scaling of the second term is consistent with that of the DP scheme with no loss derived at the end of Sec. IV. In the limit of very large κ, the last term ϱ dominates and puts an upper bound on the achievable squeezing, which is precisely the shot-noise contribution from atoms which effectively are not involved in the squeezing process. This result for nonoverlapping beams in the cold-atom case is consistent with that in Ref. [36], where nonuniform atom-light interaction also leads to an atomic-shot-noise term in squeezing. If ϱ is

small enough (ϱ here is of the order of 10^{-2}), one can neglect the effects of atom-light entanglement in our scheme, and thus the evolution of the spin system is effectively reduced to two types: (i) OAT evolution in the IR and (ii) free evolution outside the IR. In the vapor cell case, atoms enter and exit from the IR many times during the interaction process (for instance, in the above example an atom on average traverses the IR 60 times). There are about $M = C_{N_{\mathrm{at}}}^{\Xi}$ kinds of collective spins that appear in the IR, where $\Xi = \frac{1+\varrho}{1+2\varrho}N_{\mathrm{at}}$ denotes the number of atoms in the IR. For simplicity, we assume that each kind of collective spin experiences an evolution in the IR of the same time duration $o\tau_0 = T/M$ (where $o = m/M$ is an integer). Consequently, the time evolution operator for atoms can be derived,

$$U = e^{-i\gamma J_{\Xi_1,z}^2} e^{-i\gamma J_{\Xi_2,z}^2} \cdots e^{-i\gamma J_{\Xi_M,z}^2}$$

$$= e^{-i\gamma\left(C_{N_{\mathrm{at}}-1}^{\Xi-1}\sum_{i=1}^{N_{\mathrm{at}}} j_{i,z}^2 + 2C_{N_{\mathrm{at}}-2}^{\Xi-2}\sum_{i,k=1,i\neq k}^{N_{\mathrm{at}}} j_{i,z}j_{k,z}\right)}, \quad \text{(C4)}$$

where we have defined $\gamma = (1-\varrho)\frac{\sqrt{3}}{4M}\chi^2$, and $J_{\Xi_i,z}$ represents the z component of the ith collective spin, while $j_{i,z}$ denotes the z component of the ith atom. Still, for small ϱ, Eq. (C4) can be approximately expressed as $U \approx e^{-i\sqrt{3}(1-2\varrho)\chi^2/4J_z^2}$, which shows that the fast ballistic motion averages out the differences in the light-atom interaction and reduces the coupling strength by an amount proportional to ϱ.

---

[1] L.-M. Duan, J. I. Cirac, P. Zoller, and E. S. Polzik, Quantum Communication Between Atomic Ensembles using Coherent Light, Phys. Rev. Lett. **85**, 5643 (2000).

[2] K. Hammerer, A. S. Sørensen, and E. S. Polzik, Quantum interface between light and atomic ensembles, Rev. Mod. Phys. **82**, 1041 (2010).

[3] B. Julsgaard, J. Sherson, J. I. Cirac, J. Fiurasek, and E. S. Polzik, Experimental demonstration of quantum memory for light, Nature **432**, 482 (2004).

[4] D. J. Wineland, J. J. Bollinger, W. M. Itano, F. L. Moore, and D. J. Heinzen, Spin squeezing and reduced quantum noise in spectroscopy, Phys. Rev. A **46**, R6797 (1992).

[5] G. Santarelli, Ph. Laurent, P. Lemonde, A. Clairon, A. G. Mann, S. Chang, A. N. Luiten, and C. Salomon, Quantum Projection Noise in an Atomic Fountain: A High Stability Cesium Frequency Standard, Phys. Rev. Lett. **82**, 4619 (1999).

[6] C. Roos, M. Chwalla, K. Kim, M. Riebe, and R. Blatt, 'Designer atoms' for quantum metrology, Nature (London) **443**, 316 (2006).

[7] M. Kitagawa and M. Ueda, Squeezed spin states, Phys. Rev. A **47**, 5138 (1993).

[8] J. Ma, X. G. Wang, C. P. Sun, and F. Nori, Quantum spin squeezing, Phys. Rep. **509**, 89 (2011).

[9] I. D. Leroux, M. H. Schleier-Smith, H. Zhang, and V. Vuletić, Unitary cavity spin squeezing by quantum erasure, Phys. Rev. A **85**, 013803 (2012).

[10] M. H. Schleier-Smith, I. D. Leroux, and V. Vuletić, Squeezing the collective spin of a dilute atomic ensemble by cavity feedback, Phys. Rev. A **81**, 021804 (2010).

[11] I. D. Leroux, M. H. Schleier-Smith, and V. Vuletić, Implementation of Cavity Squeezing of a Collective Atomic Spin, Phys. Rev. Lett. **104**, 073602 (2010).

[12] N. Behbood, G. Colangelo, F. Martin Ciurana, M. Napolitano, R. J. Sewell, and M. W. Mitchell, Feedback Cooling of an Atomic Spin Ensemble, Phys. Rev. Lett. **111**, 103601 (2013).

[13] T. Takano, M. Fuyama, R. Namiki, and Y. Takahashi, Spin Squeezing of a Cold Atomic Ensemble with the Nuclear Spin of One-Half, Phys. Rev. Lett. **102**, 033601 (2009).

[14] J. G. Bohnet, K. C. Cox, M. A. Norcia, J. M. Weiner, Z. Chen, and J. K. Thompson, Reduced spin measurement back-action for a phase sensitivity ten times beyond the standard quantum limit, Nat. Photon. **8**, 731 (2014).

[15] O. Hosten, N. J. Engelsen, R. Krishnakumar, and M. A. Kasevich, Measurement noise 100 times lower than the quantum-projection limit using entangled atoms, Nature **529**, 505 (2016).

[16] M. Takeuchi, S. Ichihara, T. Takano, M. Kumakura, T. Yabuzaki, and Y. Takahashi, Spin Squeezing Via One-Axis Twisting with Coherent Light, Phys. Rev. Lett. **94**, 023003 (2005).

[17] C. M. Trail, P. S. Jessen, and I. H. Deutsch, Strongly Enhanced Spin Squeezing Via Quantum Control, Phys. Rev. Lett. **105**, 193602 (2010).

[18] K. Helmerson and L. You, Creating Massive Entanglement of Bose-Einstein Condensed Atoms, Phys. Rev. Lett. **87**, 170402 (2001).

[19] W. Huang, Y.-L. Zhang, C.-L. Zou, X.-B. Zou, and G.-C. Guo, Two-axis spin squeezing of two-component Bose-Einstein condensates via continuous driving, Phys. Rev. A **91**, 043642 (2015).

[20] M. Zhang, K. Helmerson, and L. You, Entanglement and spin squeezing of Bose-Einstein-condensed atoms, Phys. Rev. A **68**, 043622 (2003).

[21] Y. C. Liu, Z. F. Xu, G. R. Jin, and L. You, Spin Squeezing: Transforming One-Axis Twisting into Two-Axis Twisting, Phys. Rev. Lett. **107**, 013601 (2011).

[22] I. Bouchoule and K. Mølmer, Spin squeezing of atoms by the dipole interaction in virtually excited Rydberg states, Phys. Rev. A **65**, 041803(R) (2002).

[23] T. Fernholz, H. Krauter, K. Jensen, J. F. Sherson, A. S. Sørensen, and E. S. Polzik, Spin Squeezing of Atomic Ensembles Via Nuclear-Electronic Spin Entanglement, Phys. Rev. Lett. **101**, 073601 (2008).

[24] T. Takano, M. Fuyama, R. Namiki, and Y. Takahashi, Continuous-variable quantum swapping gate between light and atoms, Phys. Rev. A **78**, 010307 (2008).

[25] D. J. Wineland, J. J. Bollinger, W. M. Itano, and D. J. Heinzen, Squeezed atomic states and projection noise in spectroscopy, Phys. Rev. A **50**, 67 (1994).

[26] K. Hammerer, E. S. Polzik, and J. I. Cirac, Teleportation and spin squeezing utilizing multimode entanglement of light with atoms, Phys. Rev. A **72**, 052313 (2005).

[27] This assumption is feasible, since $d_{1,2}$ in reality is normally of the order of nanoseconds, while $1/\Omega$ involved here is of the order of milliseconds.

[28] L. B. Madsen and K. Mølmer, Spin squeezing and precision probing with light and samples of atoms in the Gaussian description, Phys. Rev. A **70**, 052324 (2004).

[29] Reflection loss by the first wall is neglected since it can be compensated by using a more intensive coherent state. Also, for simplicity we set $\epsilon \sim r_0$.

[30] B. Julsgaard, Quantum Memory and Teleportation Using Macroscopic Gas Samples, Ph.D. thesis, Aarhus University (2003).

[31] K. Hammerer, E. S. Polzik, and J. I. Cirac, High-fidelity teleportation between light and atoms, Phys. Rev. A **74**, 064301 (2006).

[32] G. Vasilakis, H. Shen, K. Jensen, M. Balabas, D. Salart, B. Chen, and E. S. Polzik, Generation of a squeezed state of an oscillator by stroboscopic back-action-evading measurement, Nat. Phys. **11**, 389 (2015).

[33] J. Sherson, A. S. Sørensen, J. Fiurášek, K. Mølmer, and E. S. Polzik, Light qubit storage and retrieval using macroscopic atomic ensembles, Phys. Rev. A **74**, 011802 (2006).

[34] C. A. Muschik, E. S. Polzik, and J. I. Cirac, Dissipatively driven entanglement of two macroscopic atomic ensembles, Phys. Rev. A **83**, 052312 (2011).

[35] C. A. Muschik, K. Hammerer, E. S. Polzik, and J. I. Cirac, Efficient quantum memory and entanglement between light and an atomic ensemble using magnetic fields, Phys. Rev. A **73**, 062329 (2006).

[36] J. Z. Hu, W. L. Chen, Z. Vendeiro, H. Zhang, and V. Vuletić, Entangled collective-spin states of atomic ensembles under nonuniform atom-light interaction, Phys. Rev. A **92**, 063816 (2015).